Al-Khwarizmi Engineering Journal, Vol. 6, No. 1, PP 69-79 (2010)

Al-Khwarizmi Engineering Journal

The Effect of Mechanical Combined Contact Stress with Buckling Load on the Stress Distribution in the Ball and Socket Joint Mechanism

Fathi AL Shamaa **Fatima Salman**

Department of Mechanical Engineering/ College of Engineering/ University of Baghdad

(Received 30 April 2008; accepted 17 September 2009)

Abstract

The design of components subjected to contact stress as local compressive stress is important in engineering application especially in ball and socket Joining. Two kinds of contact stress are introduced in the ball and socket joint, the first is from normal contact while the other is from sliding contact. Although joining two long links (drive shaft in steering cars) will cause the effect of flexural and tensional buckling stress in hollow columns through the ball and socket ends on the failure condition of the joining mechanism. In this paper the consideration of the combined effect of buckling Load and contact stress on the ball and socket joints have been taken, epically on the stress distribution in the contact area. Different parameters have been taken in the design of joint. This is done by changing the angles for applied loads with the principle axis, the angle of contact between ball and socket and using different applied loads.

The problem has been solved using analytical solution for computing the critical loads and using these loads for calculating the stress distribution with finite element method using ANSYS 10. The numerical results have been compared with the experimental method using photo elasticity pattern which shows good agreement between experimental and simulation results.

Keywords: *Joining, contact stress, ball and socket, buckling stress, sliding contact stress*

1. Introduction

Two major problems are introduced in the designing of joints.

1) To find the suitable length and cross sectional area for the two rods which must be jointed.
2) The kind of the joint that can sustain the condition of loading which is applied at these two rods. The first problem must be solved by calculating the buckling stresses in long rods that are subjected to compressive load. Some time failure by buckling is reached before the yield stress in compression. The buckling occurs owing to one or more of the following reason:
   a) The strut may not be perfectly straight
   b) The load may not be applied exactly along the axis.
   c) One part of the material may yield in compression more than the others.

The second problem depends on the value of the contact stress in the end of the joints. The local compressive contact stress between two joining surfaces lead to infinite values which must be avoided by increasing the bearing area reducing the value of the compressive stress to some finite value . The use of the ball and socket joints for driving members has increased considerably over the last 20 years due to their ease of use and speed of installation (i.e. the drive shaft in steering system of the automobile) which needs more suitable joint. Most of the work concentrated on determining the critical load that caused failure to the joint with different boundary conditions. Carretero J. A. et al [1] utilized two and three degree of freedom joints to connect the robot arms, with universal joints commonly used for the 2 Degree of freedom joints they have led to practical implementation of spherical joints mechanism. Alecp. Robertson et al [2] have developed a spherical joints based on a ball and

socket configuration for parallel kinematic machines; four prototypes are implemented using point, rolling sliding contact mechanism between the ball and the socket. Foully A. Mohamad et .al [3] have stated the effect of bulging and buckling stresses on the defects concentrated in wall splitting of ball and socket joint; they also stated the influence of the ratio of ball diameter to the thickness of the flang on the radial flanging force and on the failure of the joint. Erin Renee Roberts [4] used finite element software package which calculated the elastic flexural - torsional buckling load of plane frame.

This program is refractory into object -oriented design to improve the structure of the soft ware and increase its flexibility. F. Liu. et al [5] analyzed the stress distribution and the transient-elasto hydrodynamic lubrication for typical metal – on metal bearing under dynamic operation condition of load and sped for ball and socket joints . In this research, the combined effect of buckling stress with the contact stresses on the stress distribution in ball and socket joint. This analysis have accomplished numerically using finite element method ANSYS (10) comparing the experiment methods using photo elasticity. The objective of this paper is to find the critical loads from combined buckling and contact stresses which causes failure to the joint under complex condition and then to apply these loads to the region of high stress and solve them using finite element method ANSYS (10) and compare the results with the experimental one using photo elasticity pattern for ball and socket joint .

2. Theoretical Analysis

(i) Normal Buckling Stress

The global (Euler) mode occurs in slender columns and involves sudden lateral deflection without deformation of the cross section. The Euler buckling equation is (10):

$$Pcr = \frac{(EI)}{(K\ell/\pi)^2} \quad \ldots (1)$$

where EI is the bending stiffness, (l) is column length, K is the end restraint coefficient. When the length of the column is such, the predicted local and global loads are close to the experimental failure loads, which are lower than the theoretical prediction. An empirical equation was proposed by Barbero et al (q) (2000); the column buckling load is predicted as

$$Pc = Ki\ P_L \quad \ldots (2)$$

where:

$$Ki = k\lambda - \sqrt{k\lambda^{\,2} - \frac{1}{c\lambda^{\,2}}} \quad \ldots (3)$$

$$k\lambda = \left(1 + \frac{1}{\lambda^{\,2}}\right) / 2C$$

C is the empirical interaction constant adjusted to fit data determined from column test [9].

$$\lambda = \frac{KL}{\pi}\sqrt{\frac{P_L}{EI}} \quad \ldots (4)$$

The average buckling stress for a pin – ended column is:

$$\sigma_1 = \frac{P_L}{A} \quad \ldots (5)$$

where A is the cross sectional area

(ii) Lateral Bucking Area

The end supports of beam allow rotation in the plan of depth but restrict displacement of the beam ends under unstable conditions as shown in Fig. (1), the compressive side of beam depth will be laterally displaced. The beam is subjected to bending moment

$M_x = M_o \cos \Phi$, $My = M_o \sin \Phi$

And twisting moment

$M_t = M_o \cos \Phi \sin \varphi$ as shown in fig (2) from (11)

$$\frac{ELy}{Mo}\frac{\partial u^2}{\partial z^2} + \frac{Mo}{GIt}\frac{\partial u}{\partial z} = 0 \quad \ldots (6)$$

Which yields from the boundary condition
at Z=0: U =0 and Φ = 0 ,
at Z = l : U = 0 and Φ = 0
gives:

$$(Mo)cr = \frac{\pi}{\ell}\sqrt{ELyGIt} \quad \ldots (7)$$

And from equation (7), the stress lateral backling causes a tension equal to :

$$\sigma_2 = \frac{(M_o)cr \cdot y_{max}}{I}$$

$$(Mt)_{max} = Mo\psi = Mou_{\ max}\frac{\pi}{\ell} \quad \ldots (8)$$

$$\therefore \tau\,max = \frac{(Mt)max}{It} \quad \ldots (9)$$

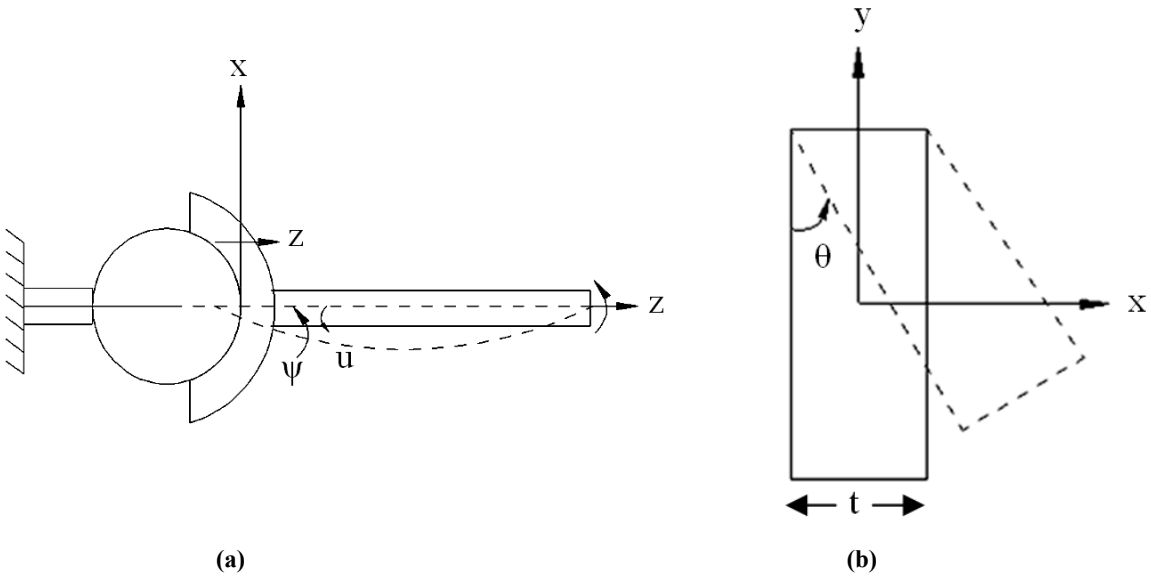

(a) **(b)**

Fig.1. Lateral Bucking of a Thin Beam in Bending.

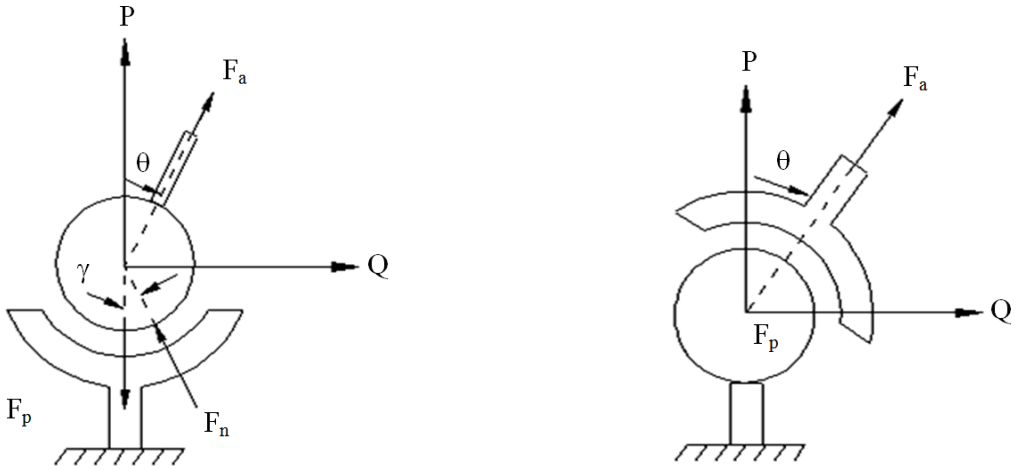

(a) Ball – Fixed and Socket – Fixed Configuration.

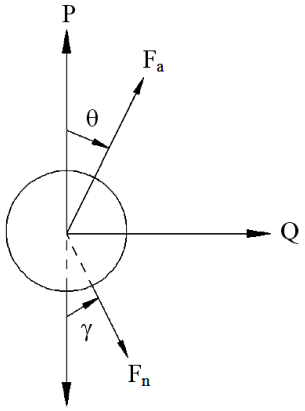

(b) Free Body Diagram of Ball Forces the Preload Force Fp Acts Along the Socket Axis.

Fig.2. Illustration of Applied Loading and Moment at the End of the Lever.

(iii) Combined Normal and Lateral Stress

For elastic condition under combined normal and shear stress, and by using $\sigma_t = \sigma_1 + \sigma_2$ tresca yields criteria for the elastic failure

$$\sqrt{\sigma_t^2 + 4\tau_{max}^2} \leq \sigma y$$

So that the proper load of P_c must be suitable for combined lateral and bending backling.

(iv) Contact Stress

Normal contact stresses the general solution in the case of asymmetrical complete contact over the range $-b \leq X \leq b$ as shown in fig (2) and is given by (12) inverse of the singular integral equation :

$$P(X) = -\frac{1}{\pi\sqrt{(b-x)}} \times \left[\int_{-b}^{b} P_c - \frac{E^*}{2}\int_{-b}^{b} \frac{h'(t)\sqrt{(b^2-t^2)}}{t-x}\,dt\right] \quad \ldots (10)$$

Where:

$$\frac{1}{E^*} = \frac{1}{E1}(1-v_1^2) + \frac{1}{E2}(1-v_2^2)$$

$$h'(x) = \begin{cases} -(a+x)/R & -b \leq x \leq a \\ 0 & -a \leq x \leq +a \\ -(x-a)/R & +a \leq x \leq b \end{cases}$$

For Hertzien Case

(v) Partial Slip Contact

In particular, the normal load p will cause normal contact while the tangential force Q will cause sliding and slip contact. This analysis is applied only to the case where the contact arises between elastically similar components. An integral equation is to be considered which relates the displacement parallel with surface to the surface tractions (ref 7) is to be considered:

$$\frac{E^*}{2} g'(x) = \frac{1}{\pi}\int_L \frac{q(\xi)d\xi}{x-\xi} + Bp(\xi) \quad \ldots (11)$$

where: g(x) is the relative tangential displacement of surface particles.

$$g'(x) = \frac{dy(\infty)}{dx}$$

Then tangential equilibrium will be satisfied if

$$Q = \int_L q(\xi)d\xi \quad \ldots (12)$$

The contact area (L) , is affected by the position of the applied normal load which has an angle θ with respect to the main axis of the ball joint represented when we find the critical load (P_c) and the contact angle (γ) which have an effect on the contact area between the clamped rod and the ball joint which varies between $180^o \rightarrow 270^o$ as shown in Fig. (2); then this effect will reduce the partial slip contact.

This problem made the contact area L very complicated, and to solve it, the value of θ obtained from eq. (12) with normal contact load P(x) must not exceed the shear yield stress of the ball and socket joint material.

(vi) Accuracy of the Mathematical Model

Two effects have been pronounced in the mathematical model that must be solved in this research.

1. The general solution in the case of asymmetrical complete contact is given by the equation of Mushkelishili's which differs from hertizian contact law and more complicated because the integral boundary condition at both P(b) and P(-b) must be zero which reduces the general solutions for a contact over the range $-b \leq x \leq b$.
   This can be revived with hertizian pressure for a completed contact i.e. in the case a/b = 0 while with a/b > 0 then the pressure in this case will be affected by the forces of the slip contact with the buckling load which will increase the slip contact rather than the normal contact which causes fatling of the contact area. The pressure distribution will be higher than the hertizian pressure especially for the inclined load with y axis which causes failure in this region.
2. The second difficult in the theoretical calculation is to find the critical buckling load which is either from banding buckling or shearing buckling and this depends on the cross sectional area of the column and in the ratio of the length of the rod to the width of the flatning end of the joint; it can be seen that the critical buckling land will be caused by shearing buckling rather than by bending buckling which will increase the slip contact and decrease the normal contact so that the

values of pressure distribution have values higher than that of hertizian law and more suitable to the stress distribution .

(vii) Finite Element Analysis

The ANSYS Finite Element Analysis (FEA) program offers variety of elements designed to treat cases of changing mechanical contact between the parts of different faces that cannot be assumed negligible. There is a number of steps in the solution procedure using the finite element packages which require the user to go through these step as shown in fig (3). Contact elements can be grouped into four general categories based on increasing the levels of sophistication of complexity

A- point to point gup elements
B- point to line (or slide line) contact element
C- point to surface contact elements
D- Surface to surface contact elements to optimize the simulations, parametric study is needed during the study different element types, element sizes, sheet length have been tried. The main objective in this effort is to reduce the required CPU time in the (ANSYS 10) solution.

Ansys Mechanical Interactive
Sleet Element 1 - Plane 2D 182 2 - Contac 172 3 - Target 169
Select Real Constant for Contact Element
Select Material Property in Elastic State for the Ball and Socket
Great The Modelgeometrics (Two Circular Contact Joint)
Mesh the Areas With Asu1table Grid
Set the Boundary Condition for Sliding and Buckling Analysis Options
Great the Load Step Files From the Theoretical Analysis
Solve the Problem to Find the Stress Distribution With Different Angle of Contact
Finish

3. Experimental Method

In this study, design of ball and socket joint is analyzed. They have been modeled and described under different type of loading, angle of contact and different shapes. The models of three types of contact angles 180°, 220° , 270° manufactured from sheets of epoxy resin MY 750 photo elastic material which has fringe constant 0.44 [M pa / (fr / mm)] circumferential ball and socket joint . The models wave machined from proto type preparation using milling machine. The profile and external dimensions are all exactly 2.5 times the size of the original to facilitate handling and data collection. This model was a two dimensional component as the loading required for these models to be axially , -10 °, -20°than special loading frame required. After the first loading , the ball and socket of the specimen was placed in a dark - field circular which has been used to view in plane Polaris cope and the point is located by rotating the ball with fixed socket until the isoclinic contour is perpendicular to the contact face . The point at which this occurred was marked and the ball and socket were removed from the poloriscope and then it was repeated for another loading.

4. Discussion of Results

In this research the results illustrate the variation Of the normal contact stress which has been solved By ANSYS 10 with different loading. The sample used in the numerical and experimental procedure is a ball joint of a radius equal (5 cm) and a socket of width (2 cm) and length (20 cm). All the applied load is on the fixed ball and the moving socket at angle 10°, and 20° as shown in fig (l). It can be seen that with increasing the angle of the applied load, the normal stress will be decreased. Also it can be seen from fig (2) that the variation of slip contact stress with different loading and the behavior of the slip contact stress which increases with increasing the angle Φ. These two effect of contact stresses will give different values when combined with the buckling stress which increased very high at angle Φ = 20. Figures 4 to 9 it show increasing in the value of normal contact stress with increasing the angle of contact of 180° , 220° and 270°. The sliding contact stress will have max effect at 270 ° and this is because the value of contact stress will be affected by this reduction. Figures (13) and (14) illustrate the experimental results of combined contact and

buckling stress with the applied load sat 180° and 270° which shows good agreement with the numerical one.

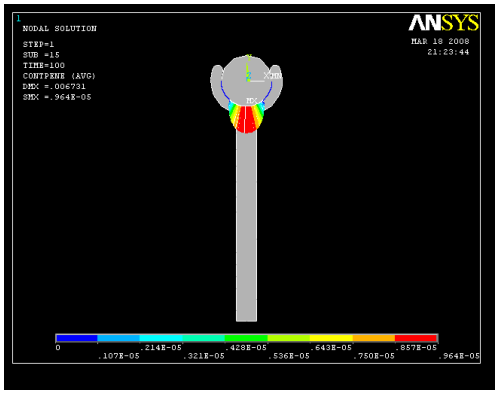

Load (10 N), Φ = 180º

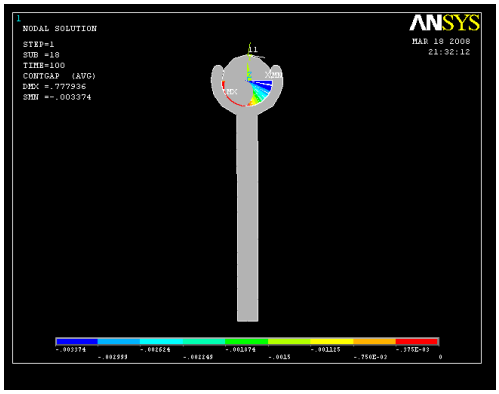

Load (10 N), Φ = 180º

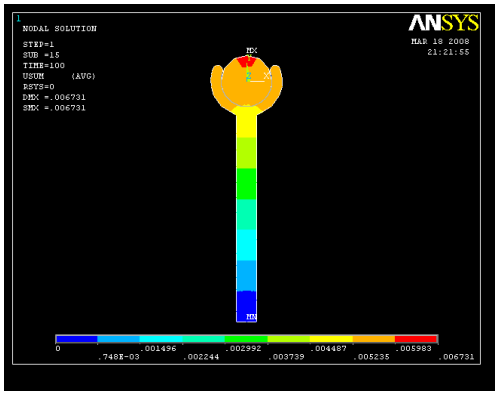

Load (10 N), Φ = 220º

Load (10 N), Φ = 220º

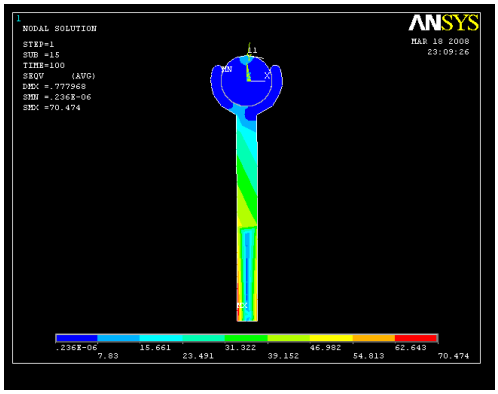

Load (10 N), Φ = 270º

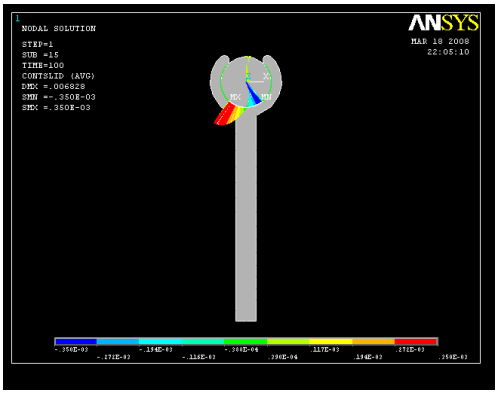

Load (10 N), Φ = 270º

Fig. 3. The Experimental Results of ANSYS 10 for the Pattern of Contact Angle 180º, 220º and 270º Respectively.

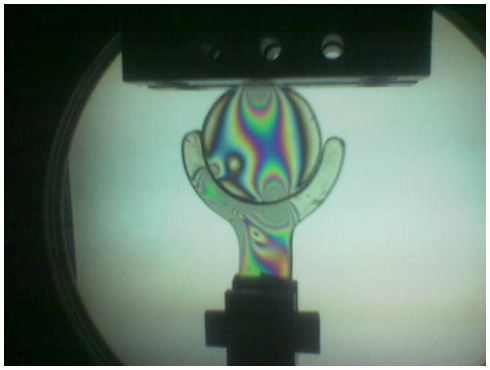

Load (1.5 N), Φ = 0

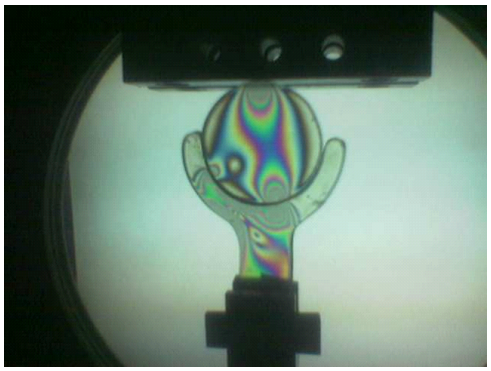

Load (1.5 N), Φ = 0

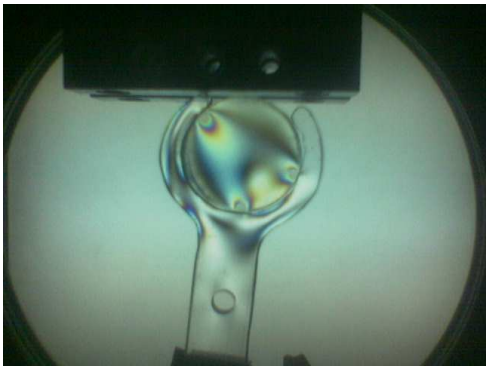

Load (2 N), Φ = 10

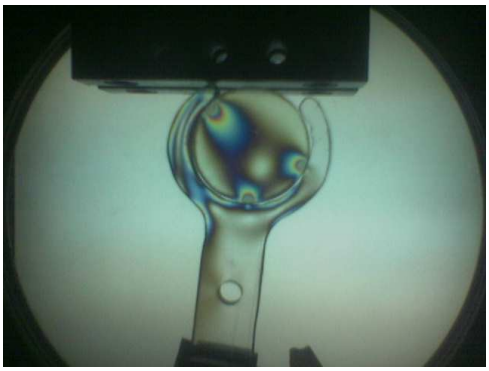

Load (2 N), Φ = 10

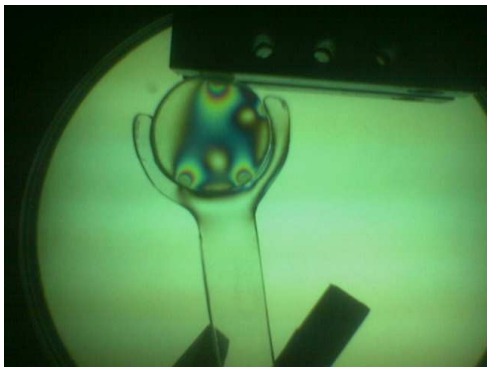

Load (1N), Φ = 20

Light

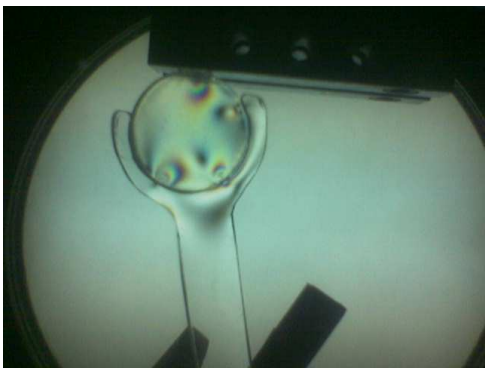

Load (1N), Φ = 20

Dark

Fig.4. Shows the Experimental Photo Elasticity Pattern Using Light and Dark Field to Show the Normal and Shear Slip Stresses in Different Contact Angle.

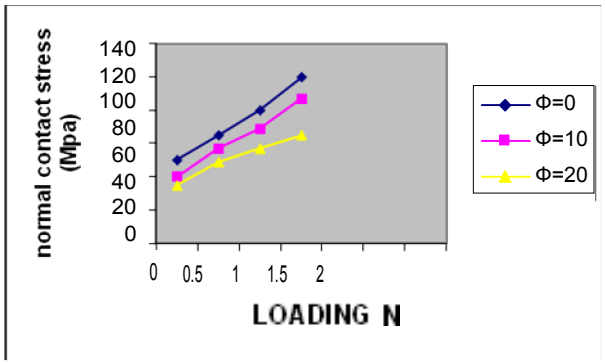

Fig.5. The Variation of Normal Contact Stress Numerically with the Loading at 180° Angle of Contact.

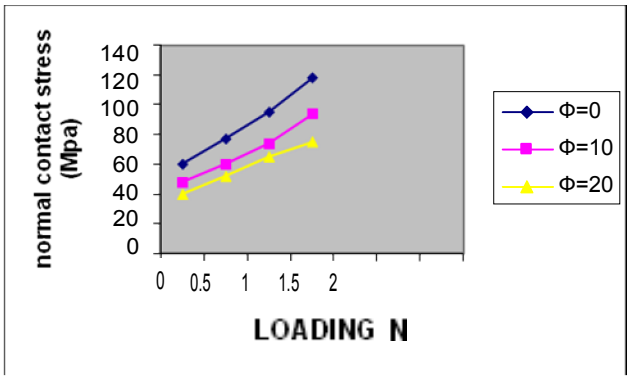

Fig.8. The Variation of Normal Contact Stress Numerically With the Loading at 220° Angle of Contact.

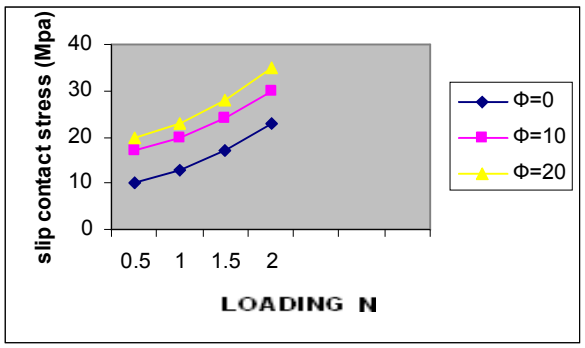

Fig.6. The Variation of Slip Contact Stress Numerically With the Loading at 180° Angle of Contact.

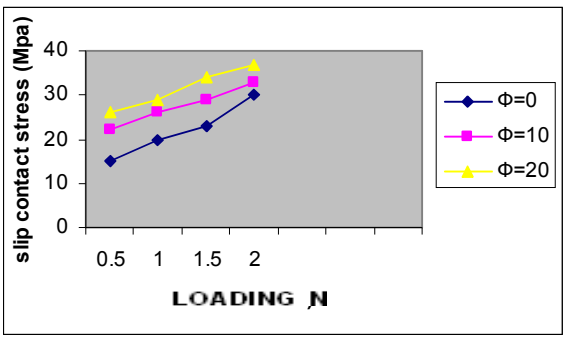

Fig.9. The Variation of Slip Contact Stress Numerically With the Loading at 220° Angle of Contact.

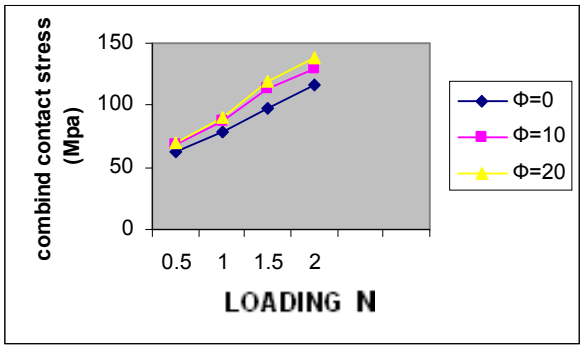

Fig.7. The Variation of Combined Contact and Buckling Stress Numerically with the Loading at 180° Angle of Contact.

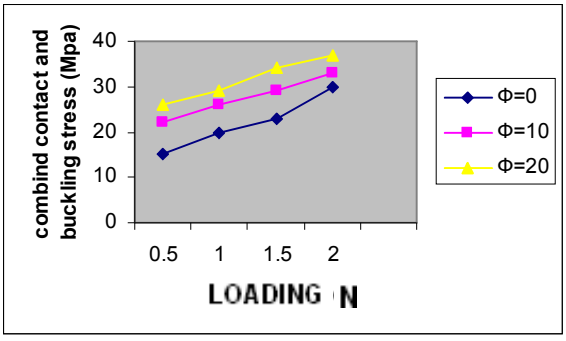

Fig.10. The Variation of Combined Contact Stress Numerically With the Loading at 270° Angle of Contact.

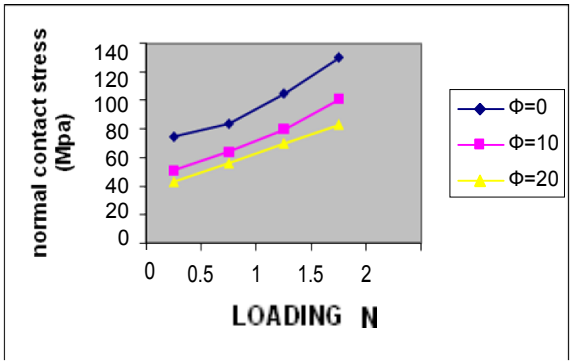

Fig.11. The Variation of Normal Contact Stress Numerically With the Loading at 270° Angle of Contact.

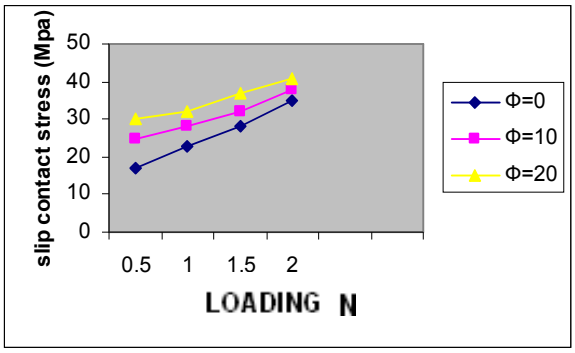

Fig.12. The Variation of Slip Contact Stress Numerically With the Loading at 270° Angle of Contact.

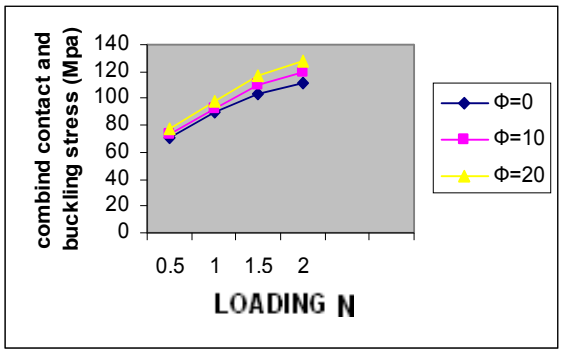

Fig.13. The Variation of Combined Contact and Buckling Stress Numerically With the Loading at 270° Angle of Contact.

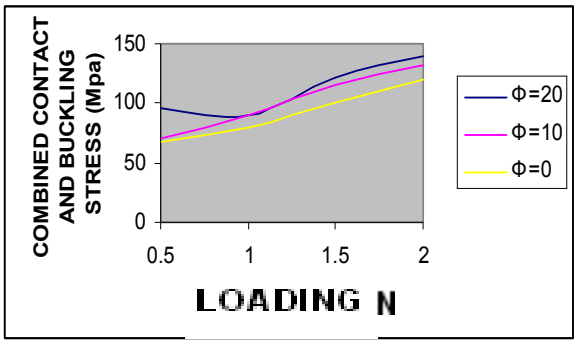

Fig.14. The Variation of Combined and Buckling Stresses Experimentally With the Applied Loading at 180° Angle of Contact.

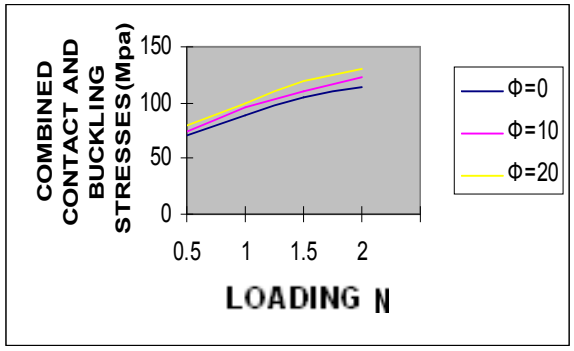

Fig.15. The Variation of Combined and Buckling Stresses Experimentally With the Applied Loading at 270° Angle of Contact.

5. Conclusions

The problem of ball and socket joint failure with combined effect of buckling and contact stresses has been studied, giving results for surface traction and interior stress field induced by contact. This research was solved numerically using ANSYS (10) and the results were compared with the experimental one using photo elasticity which gives good illustration about stress distribution and the effect of sliding and normal contact on the length of the joining rods at different angle of contact. The numerical results give good agreement with the experimental one.

The results show that the buckling load in the ball joint will be affected on the contact pressure distribution which causes the shear buckling to flatten the contact area of the joint and this causes the pressure distribution to be higher than the horizontal pressure. The angle of inclination of the contact rod with the ball joint will increase under large inclined angle of the rod and this causes the

pressure distribution of the contact area to double more than the value of the Hertizian law.

Nomenclature

E_i	Young's modulus of body i N / m^2
I	Second moment of area m^4
k	The end restraint coefficient
l	Column length m
G	Modulus of rigidity N / m^2
A	Cross sectional area mm^2
P_L	Short – Column load N
C	Empirical interaction constant
$(M_o)_{cr}$	The critical end bending moment Nm
σ_1	Normal bucking stress M la
M_t	The twisting moment N.m
τ_{max}	The maximum tensional shear stress at U_{max} MPa
σ_2	The stress of lateral bucking MPa
σ_y	Yield stress of the joint material MPa
L	Contact area related to the geometry of the contacting surfaces mm^2
a	The straight part of punch boundary length mm
b	The end of the contact length ($b \leq x \leq -b$) mm
$h(\hat{b})$	The slope at each point of the profile of the ball joint flaunting
t	A small region from the contact length specified by the angle ψ
R	The corners arc of contact mm
B	Lundurs second constant which is equal to zero to elastically similar contact
q	Slip shearing traction force N
Q	Tangential shearing force N

6. Reference

[1] Carretero J Apodorodeski RP,Nahon MA. Gosselincm.Kinematic "Analysis and optimization of a new three –degree of – freedom spatial parallel manipulator ". ASME J Mech Des 2000, 122(1): 17-24

[2] Aleep. Robertson and Alexander H.Slocum "Measurement and characterization of precision spherical joint".

[3] Foully A. Mohammed, Samy Zein El –Abden, Mohi Eldeen Abdel – Rahman, " A rotary flange , forming process on the lath using a ball –shaped ,mater. Process .technol, 2004.

[4] Erin Renee Roberts, (2002) " Elastic flexural-torsional buckling analysis using finite element method" . University of pittsburghat Johnstown.

[5] F.LIU, Z.M.JIN,F.hirt, c.rieker, p. Roberts and p.grigoris . "Transient elasto hydrodynamic lubrication analysis of metal – on- metal hip implautunder simulated walking conditions.

[6] ANSYS INC V 10', ' ANSYS Manual, 2005.

[7] E.J. Hearn, (1985) "Mechanics of Material", Vol. 2, pergamon press comp, London and Northampton.

[8] Mc Master – Carr , Catalog , 473 Ridge road , Dayton , NJ08810 , USA , 2000 .

[9] Barbero, E.J., Dede, E and Jones, S., "Experimental verification of bucking mode interaction in intermediate length columns ", I. J. Solid Structures, 2000.

[10] S. Timoshinko , " Theory of elasticity stability " , 1975 .

[11] Abdel – Rahman Ragab, Salah Eldin Bayoumi, " Engineering solid mechanics fundamentals and applications " . CRC Press LLC, 2000.

[12] M. Ciavarella, D.A Hills and G. Monno, "The influence of rounded edges on indentation by a flat punch ". Proc. Inst. Mech. Engrs. Vol 212 Partc P 319, 1998.

التأثير الميكانيكي المشترك لإجهادات وأحمال الانبعاج على توزيع الإجهادات في المفصل نوع الكرة والمقبض

فتحي الشماع فاطمة سلمان
قسم هندسة الميكانيك/ كلية الهندسه/ جامعة بغداد

الخلاصة

إن تصميم الأجزاء الميكانيكية التي تخضع إلى إجهادات تلامس موضعي مثل الإجهادات الموضعية المضغوطة يكون مهماً جداً في التطبيقات الهندسية وخصوصاً في المفاصل نوع الكرة والمقبض الذي يتضمن نوعين من إجهادات التلامس تظهر في مفصل الكرة والمقبض ، الأول التلامس العمودي والآخر التلامس الإنزلاقي.

خصوصاً عند ربط موصلين طويلين كما في عمود التدوير في مقود السيارة بسبب التأثير المشترك لإجهادات الانبعاج الالتوائي في الأعمدة المجوفة خلال نهايات الكرة والمقبض إلى فشل آلية الربط الميكانيكية .

هذا البحث أخذ بنظر الاعتبار التأثير المشترك لحمل الانبعاج وإجهادات التلامس في مفصل الكرة والمقبض على توزيع الإجهادات في منطقة التلامس . رموز مختلفة أخذت في تصميم المفصل وذلك بتغيير زاوية الأحمال المسلطة مع المحور الأساسي وباستخدام أحمال مسلطة مختلفة.

هذه المشكلة عولجت باستخدام الحلول التحليلية بحساب الأحمال الحرجة من عملية الانبعاج والتلامس واستخدام هذه الأحمال لحساب توزيع الإجهادات باستخدام الطريقة المتطورة (ANSYS 10) . النتائج العددية قورنت مع النتائج العملية باستخدام جهاز تحليل الإجهادات وأظهرت تطابق جيد بينهم.